IAI Journals.ASM.org

Early Control of *Mycobacterium tuberculosis* Infection Requires *il12rb1* Expression by *rag1*-Dependent Lineages

Halli E. Miller and Richard T. Robinson

Department of Microbiology and Molecular Genetics, Medical College of Wisconsin, Milwaukee, Wisconsin, USA

***IL12RB1* is essential for human resistance to *Mycobacterium tuberculosis* infection. In the absence of a functional *IL12RB1* allele, individuals exhibit susceptibility to disseminated, recurrent mycobacterial infections that are associated with defects in both *RAG1*-dependent and *RAG1*-independent hematopoietic lineages. Despite this well-established association, a causal relationship between *M. tuberculosis* susceptibility and *IL12RB1* deficiency in either *RAG1*-dependent or *RAG1*-independent lineages has never been formally tested. Here, we use the low-dose aerosol model of experimental tuberculosis (TB) to both establish that infected *il12rb1*$^{-/-}$ mice recapitulate important aspects of TB in *IL12RB1* null individuals and, more importantly, use radiation bone marrow chimeras to demonstrate that restriction of *il12rb1* deficiency solely to *rag1*-dependent lineages (i.e., T and B cells) allows for the full transfer of the *il12rb1*$^{-/-}$ phenotype. We further demonstrate that the protection afforded by adaptive lymphocyte *il12rb1* expression is mediated partially through *ifng* and that, within the same infection, *il12rb1*-sufficient T cells exhibit dominance over *il12rb1*-deficient T cells by enhancing *ifng* expression in the latter population. Collectively, our data establish a basic framework in which to understand how *IL12RB1* promotes control of this significant human disease.**

Despite tremendous efforts in the past and present to control tuberculosis (TB), infection with *Mycobacterium tuberculosis* remains a significant source of global morbidity and mortality. It is widely recognized that controlling the spread of this organism will require a combination of approaches, including the education of affected populations, provision of adequate public health infrastructure, decreasing the incidence of the AIDS comorbidity, and developing novel therapies for tuberculous individuals (57). The last approach will likely depend on our understanding the basic mechanisms that have evolved to protect humans against mycobacterial infection, the genes that underlie these mechanisms, and the cell lineages in which these genes must be expressed.

Among the genes that are well established as being essential for controlling *M. tuberculosis* infection is *IL12RB1* (2–4, 15, 16). That *IL12RB1* is required for controlling mycobacterial infection was first demonstrated by Altare et al. and de Jong et al. (4, 16), who reported case studies of *IL12RB1* null individuals from Mediterranean regions who had suffered from disseminated *Mycobacterium bovis* bacillus Calmette-Guerin (BCG) infections. Since that time, the same association has been observed across multiple other ethnicities (15), demonstrating that *IL12RB1*'s influence on the dissemination of mycobacterial infections is nearly ubiquitous. *IL12RB1* encodes a minimum of two protein isoforms (56), one of which is IL-12Rβ1 (isoform 1), the type I integral membrane protein that serves as a low-affinity receptor for the p40 subunit of the cytokines interleukin-12 (IL-12), IL-23, and IL-12(p40)$_2$ (10, 47, 51, 72). To confer high affinity and biological responsiveness to the cytokine IL-12 or IL-23, IL-12 receptor β1 (IL-12Rβ1) must both physically associate with each cytokine and signal in complex with either IL-12Rβ2 or IL-23R, respectively (73). The second isoform expressed from *IL12RB1* (IL-12Rβ1ΔTM, or isoform 2) is a product of alternative splicing, lacks the transmembrane (TM) domain of IL-12Rβ1, and contains a C-terminal sequence that is unique from that of IL-12Rβ1 (11, 56, 63). Unlike isoform 1, isoform 2's contribution to IL-12 and IL-23 signaling is not yet known.

Despite *IL12RB1*'s long recognition as being important for *M. tuberculosis* control, the identification of which cell types must express *IL12RB1* for pathogen control to occur has never been formally tested. Deducing this based on mRNA expression alone is not possible since during active TB the lungs are infiltrated by multiple hematopoietic cells expressing *IL12RB1* (69), including both *RAG1*-independent cell types (e.g., NK cells and dendritic cells) and *RAG1*-dependent cell types (e.g., αβ-T cells and B cells). Here, we use an established model of experimental TB to specifically test whether *rag1*-dependent lineages must express *il12rb1* (the mouse homolog of human *IL12RB1*) for tubercular control to occur, as well as the mechanisms by which *il12rb1* promotes the same. We further determine the specific contribution T cell gamma interferon (IFN-γ) expression plays in controlling *M. tuberculosis* infection, as well as the relative dominance of *il12rb1*$^{+/+}$ versus *il12rb1*$^{-/-}$ T cells, during the same *M. tuberculosis* infection experiment as it pertains to production of IFN-γ. Our results suggest that positive regulators of T cell *IL12RB1* expression might serve as potential adjunctive therapies for tuberculosis individuals.

MATERIALS AND METHODS

Mice. Mice were bred at the Medical College of Wisconsin (MCW) in the MCW Biomedical Resource Center and were treated according to National Institutes of Health and MCW Institute Animal Care and Use Committee (IACUC) guidelines. C57BL/6, B6.129S7-*Rag1*^{tm1Mom}/J (i.e., *rag1*$^{-/-}$ mice), B6.129S7-*Ifng*^{tm1Ts}/J (i.e., *ifng*$^{-/-}$ mice), and B6.SJL-*Ptprc*^{a} *Pepc*^{b}/BoyJ (i.e., CD45.1 congenics) mice were originally purchased

Received 25 April 2012 Returned for modification 24 May 2012
Accepted 10 August 2012
Published ahead of print 20 August 2012
Editor: J. L. Flynn
Address correspondence to Richard T. Robinson, rrobinson@mcw.edu.

doi:10.1128/IAI.00426-12

from the Jackson Laboratory (Bar Harbor, ME). B6.129S1-*Il12rb1*^{tm1jm}/J (*il12rb1*$^{-/-}$) mice (74) were kindly provided by Andrea M. Cooper (Trudeau Institute, Saranac Lake, NY). IFN-γ–enhanced yellow fluorescent protein (eYFP) reporter mice (i.e., Yeti mice) (64) were kindly provided by Markus Mohrs (Trudeau Institute, Saranac Lake, NY) and Richard Locksley (Howard Hughes Medical Institute, University of California San Francisco, San Francisco, CA).

Genotyping and background analysis. *il12rb1*$^{-/-}$ mice were genotyped using primers we designed specifically for this study due to difficulties we encountered amplifying wild-type (WT) *il12rb1* with published primer sets (data not shown). Our protocol is detailed here. To screen for the presence of a wild-type *il12rb1* allele, genomic DNA (gDNA) from tail snips was isolated using the Promega Wizard SV Genomic DNA method (Promega, Madison, WI) and amplified with primers NF1 (5′-CAGAGA TCCTCCTGCCTCTG-3′) and NF2 (5′-TATGGTTCGGAGGGACAAA G-3′) in a 50-μl reaction mixture comprising 2 μl of gDNA, 1.5× NEB *Taq* buffer (from a 10× solution), 2 mM $MgCl_2$, 0.2 μM primer NF1, 0.2 μM primer NF2, 0.2 mM each deoxynucleoside triphosphate (dNTP), 5% dimethyl sulfoxide (DMSO), and 1U of *Taq* polymerase (New England BioLabs, Ipswich, MA). To screen for the knockout (KO) *il12rb1* allele, gDNA was amplified with primers NF1 (sequence above) and NF3 (5′-T GGATGTGGAATGTGTGCGAG-3′) in a 50-μl reaction mixture comprising 2 μl of gDNA, 1.0× NEB *Taq* buffer (from a 10× solution), 2 mM $MgCl_2$, 0.2 μM primer NF1, 0.2 μM primer NF3, 0.2 mM each dNTP, 5% DMSO, and 1U of *Taq* polymerase. The parameters for amplification of both wild-type and knockout *il12rb1* alleles were the following: one cycle of 95° for 5 min; 35 cycles of 95° for 30 s, 60° for 1 min, and 72° for 1 min; one cycle of 72° for 10 min. Amplicons were resolved on a 1% agarose gel using traditional electrophoresis techniques.

Prior to their being used to generate radiation bone marrow chimeras, the extent to which *il12rb1*$^{-/-}$ mice had been backcrossed to the C57BL/6 background was tested by the DartMouse Speed Congenic Core Facility at Dartmouth Medical School (Hanover, NH). DartMouse uses an Illumina, Inc. (San Diego, CA) GoldenGate Genotyping Assay to interrogate 1,449 single nucleotide polymorphisms (SNPs) spread throughout the genome. The raw SNP data were analyzed using DartMouse's SNaP-Map and Map-Synth software, allowing the determination for each mouse of the genetic background at each SNP location. This analysis demonstrated that individual *il12rb1*$^{-/-}$ imports ranged between 95% backcrossed to >98% backcrossed (data not shown). Only those mice with ≥98% C57BL/6 background were bred and, consequently, used for the generation of radiation bone marrow chimeras.

Radiation bone marrow chimeras. Bone marrow cells from either C57BL/6, *il12rb1*$^{-/-}$, *rag1*$^{-/-}$, *ifng*$^{-/-}$, or CD45.1 congenic donors were harvested via perfusion of the femur and tibia medullary cavities with complete Dulbecco's modified Eagle's medium (DMEM). Marrow suspensions were pelleted and subsequently resuspended in red blood cell (RBC) lysis buffer (155 mM NH_4Cl, 10 mM $KHCO_3$) to remove red blood cells; following RBC lysis, the marrow was washed and resuspended at 5×10^7 cells/ml in sterile phosphate-buffered saline (PBS). As indicated in Results and figure legends, for some experiments, admixtures of select marrow preparations were made after normalizing all preparations to the same cell concentration. Recipient mice received 2 × 5 Gy (500 rads) doses of whole-body irradiation 3 h apart in a Gammacell Irradiator (1,000 rads total). Immediately following the second dose, mice were injected intravenously (i.v.) with 200 μl of marrow preparation (i.e., 1×10^7 total bone marrow cells). Mice were allowed 6 weeks to reconstitute prior to their use in experiments. Two weeks prior to experimental infection, bone marrow recipients were taken off antibiotic-containing food.

Experimental infection. The H37Rv strain of *M. tuberculosis* (kindly sent to us by Andrea Cooper) was grown in Proskauer Beck medium containing 0.05% Tween 80 to mid-log phase and frozen in 1-ml aliquots at −70°C. For aerosol delivery of ~80 bacteria, animals were placed in a Glas-Col Inhalation Exposure System (Glas-Col, Terre Haute, IN) at a maximum of 20 mice per sector. After the nebulizer (Glas-Col) was loaded with 10 ml of diluted H37Rv (5×10^6 CFU/ml in deionized water), mice were infected using the following exposure settings: 900 s for warm-up, 3,600 s to nebulize, 1,800 s for cloud decay, 900 s for UV exposure (vacuum pressure, 50; compressed-air pressure, 15). Immediately after infection, mice were placed in biocontainment unit (BCU) cages and subsequently monitored during the period of infection for outward signs of distress, per IACUC oversight. Lungs from a group of control mice were plated at day 1 postinfection to confirm the delivery ~80 CFU.

Bacterial load determination. Infected mice were euthanized by CO_2 asphyxiation; lungs, spleen, and liver were aseptically removed and individually homogenized in sterile normal saline using the Gentle Macs system, program RNA1.1 (Miltenyi, Bergisch Gladbach, Germany). The Gentle Macs system was used to increase containment of infectious aerosols generated during the homogenization process; efficient homogenization using RNA1.1 was ensured by comparing our *M. tuberculosis* CFU counts to those of other investigators using a traditional polytetrafluoroethylene (PTFE) pestle/borosilicate glass tube system (personal communication, Robert North, Trudeau Institute, Saranac Lake, NY). Serial dilutions of the organ homogenate were plated on nutrient 7H11 agar. The number of mycobacterial CFU was determined after plates were incubated for 2 weeks at 37°C in 7% CO_2.

Quantitative PCR analysis. Lung RNA was extracted from infected, snap-frozen tissue by homogenizing the tissue in RLT lysis buffer (Qiagen, Germantown, MD) using the Gentle Macs system, program RNA2.1 (Miltenyi). Total RNA was extracted from the lysis solution according to the manufacturer's protocol. RNA samples from each group/time point were reverse transcribed using Fermentas reagents (Thermo Scientific, Glen Burnie, MD). cDNA was then amplified using SYBR green reagents (Fermentas) on a Bio-Rad iQ5 detection system; threshold cycle (C_T) values were determined using the Bio-Rad iQ5 bundled software (Bio-Rad, Hercules, CA). The expression levels of select mRNAs (e.g., *ifng*) relative to expression of the housekeeping gene *gapdh* were determined using the ΔC_T calculation recommended by the manufacturer. The forward (F) and reverse (R) primers used for real-time amplification of cDNA samples were as follows (5′-3′): *gapdh*, (F) CATGGCCTTCCGTG TTCCTA and (R) GCGGCACGTCAGATCCA; *ifng*, (F) TCAAGTGGCA TAGATGTGGAAGAA and (R) TGGCTCTGCAGGATTTTCATG; *tnfa*, (F) CCTGTAGCCCACGTCGTAG and (R) GGGAGTAGACAAGGTAC AACCC; *nos2*, (F) GGCAGCCTGTGAGACCTTTG and (R) GCATTGG AAGTGAAGCGTTTC; *irgm1*, (F) AGACCCATTATGCTCCCCTGA and (R) CCTGTTTGGTATGACGTGACAA.

Cell preparations. Lung cell suspensions were prepared by perfusing heparin-containing PBS through the mouse heart until the lungs appeared white, whereupon they were removed and sectioned in incomplete DMEM. Dissected lung tissue was then incubated in DMEM containing collagenase IX (0.7 mg/ml) and DNase (30 μg/ml) at 37°C for 30 min. Digested lung tissue was gently homogenized and passed through a 70-μm-pore-size nylon tissue strainer; the resultant single-cell suspension was treated with RBC lysis solution, washed, and counted. Cells prepared in this way were subsequently used for flow cytometric analyses or further magnetic purification. For collection of bronchoalveolar lavage (BAL) cells, serial inflation and flushing of the lungs (via the trachea) with 400 μl of Dulbecco's PBS (DPBS) were performed; collected cells were directly used for staining and flow cytometric analysis.

Flow cytometry. All antibodies used for flow cytometric analysis were purchased from BD Pharmingen (San Diego, CA). Lung cell preparations were washed with fluorescence-activated cell sorting (FACS) buffer (2% fetal calf serum [FCS] in PBS) and stained with antibodies recognizing either Thy1 (clone 30-H12), NK1.1 (clone PK136), CD11c (clone HL3), CD45.1 (clone A20), CD45.2 (clone HIS41), γδ-T-cell receptor (TCR) (clone GL3), CD4 (clone L3T4), CD8 (clone 53-6.7), CD19 (clone MB19-1) and Gr1 (clone RB6-IC5). Acquired data were analyzed with FlowJo software (Tree Star Inc., Ashland, OR).

For intracellular cytokine analyses, cells were collected, washed, and placed in a V-bottom, 96-well plate in complete medium with 50 ng/ml

phorbol myristate acetate (PMA; Sigma-Aldrich) and 1 μg/ml ionomycin (Sigma-Aldrich). For stimulation of NK cells, both recombinant IL-12 and IL-18 were added to select wells in addition to PMA-ionomycin. Cells were placed in a 37°C incubator for 4 h; brefeldin A (Sigma-Aldrich) was added at 5 μg/ml for the final 2 h. After cells were washed, they were fixed in 4% formaldehyde in PBS. Cells were made permeable in 0.1% saponin (Sigma-Aldrich) in PBS with 2% FCS and stained with phycoerythrin (PE)-conjugated anti-IFN-γ (clone XMG1.2). Bromodeoxyuridine (BrdU) staining was performed using a fluorescein isothiocyanate (FITC) BrdU flow kit system 2 days after intraperitoneal (i.p.) administration of BrdU (BD Pharmingen); intracellular Tbet and Foxp3 staining was similarly assessed using commercially available antibodies and reagents (BD Pharmingen) according to the manufacturer's instructions. After all staining, cells were washed twice and acquired on a biosafety cabinet (BSC)-contained Guava 8HT flow cytometer (Millipore).

Western analysis of purified lung lineages. For lineage purification and protein expression analysis of IL-12Rβ1 protein, cell preparations from *M. tuberculosis*-infected lungs (day 30 postinfection) were magnetically sorted using the Miltenyi system into either CD45-negative ($CD45^{neg}$), $CD45^+$, $I\text{-}A^{b+}$, $CD11b^+$, $Ly6G^+$, $CD11c^+$, $NK1.1^+$, or $Thy1^+$ fractions according to the manufacturer's protocols. Afterwards, cells were lysed in β-mercaptoethanol containing lithium dodecyl sulfate (LDS) sample buffer (Invitrogen) by boiling for 1 h. Denatured lysates were then run on a 4 to 12% bis-Tris gel (Invitrogen), transferred to polyvinylidene difluoride (PVDF) membrane, and blotted with polyclonal anti-mouse IL-12Rβ1 (R&D Systems). For detection, blots were probed with the appropriate horseradish peroxidase (HRP)-conjugated secondary antibody.

Histological analysis. Lungs were inflated through the trachea with 10% neutral buffered formalin, resected, and paraffin embedded; subsequently generated sections were stained with either Masson's trichrome or with carbol fuchsin (i.e., Ziehl-Neelsen stain). Once slides were generated, a histopathological analysis of each lobe was performed. Images of both trichrome and acid-fast stains were taken with a Labophot-2 upright microscope (Nikon, Tokyo, Japan) using a Retiga 2000R camera (QImaging, Surrey, British Columbia, Canada) and analyzed using NIS Elements software (Nikon).

Statistical analysis. Figures were prepared using GraphPad Prism, version 5.0a. Statistical analyses used the bundled software. Bars in the figures show means plus standard deviations (SD). Numbers shown between data points represent *P* values for the comparisons indicated on the figures. Statistical comparisons involving more than two experimental groups used analysis of variance (ANOVA). All other statistical comparisons used Student's *t* test.

RESULTS

***il12rb1* is required to control pulmonary *M. tuberculosis* infection.** *IL12RB1* null individuals display an enhanced susceptibility to mycobacterial infections that is associated with impaired lymphocyte expression of *IFNG* (16). Prior to using the low-dose aerosol mouse model of TB (48) to determine which lineages must express *il12rb1* (the mouse homolog of *IL12RB1*) for mycobacterial control to occur, it was necessary to first determine the extent to which $il12rb1^{-/-}$ mice recapitulated the phenotype of *IL12RB1* null individuals. For this, $il12rb1^{-/-}$ mice (74) were aerogenically infected with a low dose (~80 CFU) of the virulent *M. tuberculosis* strain H37Rv; at select times postinfection, lungs were assessed for bacterial burden, the presence of pulmonary pathology, and the expression of select genes known to promote tubercular control.

Consistent with historical observations using this model (46), *M. tuberculosis* burden progressively grew in wild-type mice for ~20 days, after which time growth was inhibited, and infection was held at a mostly stationary level (Fig. 1A). In contrast, *M. tuberculosis* growth in $il12rb1^{-/-}$ lungs continued to increase past 20 days to levels greater than those in wild-type controls (Fig. 1A). Regarding the localization of *M. tuberculosis* in the infected lungs, consistent with the extensive survey of Rhoades et al. (55), at day 20 postinfection acid-fast bacilli (AFB) in wild-type lungs were difficult to locate but, when found, were restricted to macrophages within inflamed alveoli (Fig. 2A). In $il12rb1^{-/-}$ mice, however, AFB could be found not only near alveoli (Fig. 2B and B and iii) but also near sites of potential dissemination, including the lung vasculature (Fig. 2Bi) and bronchioles (Fig. 2Bii). While the majority of AFB in $il12rb1^{-/-}$ lungs were macrophage associated, instances of AFB associating with both bronchiolar (Fig. 2Biia and b) and alveolar epithelial cells (Fig. 2Biii) were observed. By 50 days postinfection, bacterial burdens were nearly 100-fold

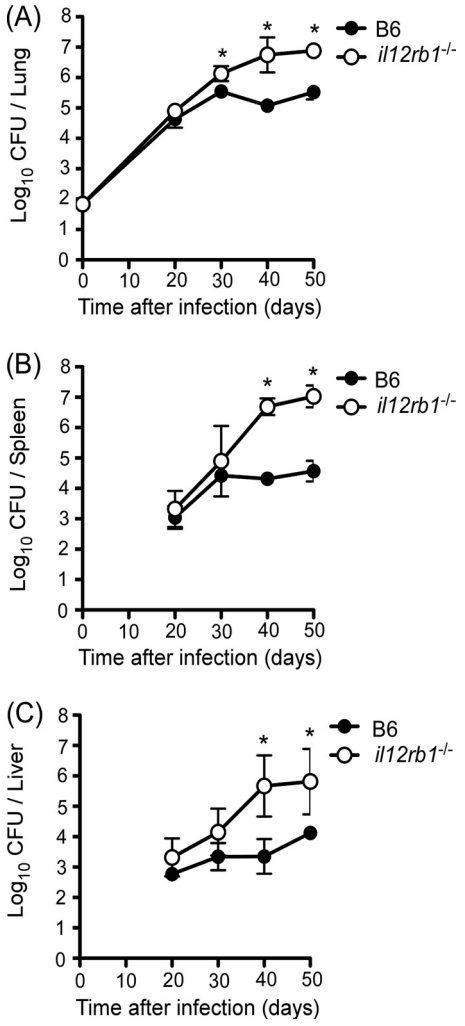

FIG 1 *il12rb1* is required to limit *M. tuberculosis* burden in multiple organs. Groups of C57BL/6 (B6) and $il12rb1^{-/-}$ mice were simultaneously infected via aerosol with ~80 CFU of *M. tuberculosis* H37Rv. At select times postinfection, *M. tuberculosis* burdens in the lungs (A), spleen (B), and liver (C) were assessed by plating serial dilutions of homogenized organs on 7H11. Shown for each time is the mean number of CFU ($\log_{10}$) present in four mice per genotype per time point. Error bars represent ±SD; asterisks indicate that a significant difference between C57BL/6 and $il12rb1^{-/-}$ mice was observed at the indicated time point (i.e., $P \leq 0.05$ as determined using Student's *t* test). This experiment was repeated four separate times, each with similar results.

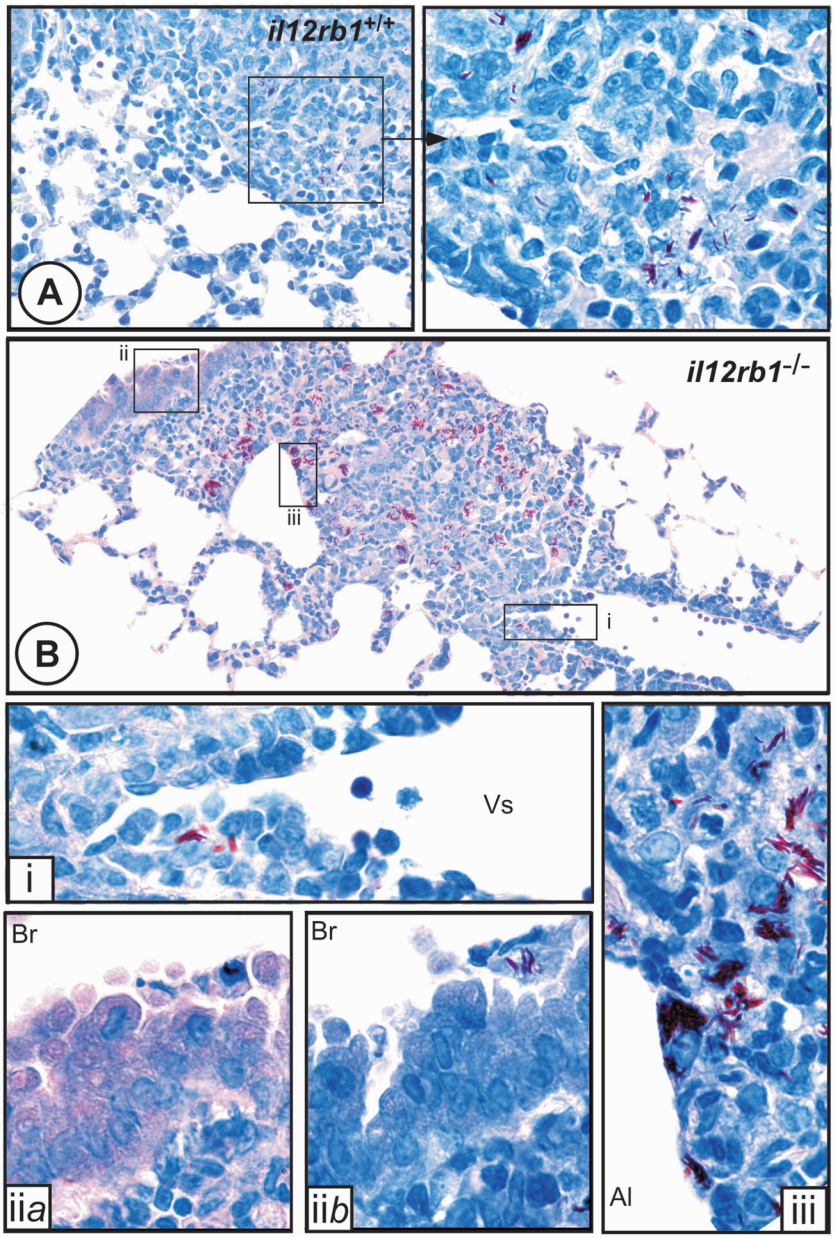

FIG 2 The localization of acid-fast bacteria in *il12rb1*$^{-/-}$ lungs is distinct from that in C57BL/6 mice. Twenty days following *M. tuberculosis* infection, lungs of C57BL/6 and *il12rb1*$^{-/-}$ mice were fixed and stained for acid-fast bacilli (AFB) in order to visualize the localization of *M. tuberculosis* in lungs of either genotype. Shown in panel A, left, is a micrograph at ×10 magnification that is representative of C57BL/6 lungs at this time; at right is a ×100 magnification of the inset indicated in the left panel showing AFB within inflamed alveoli. (B) Representative micrograph at a ×10 magnification of *il12rb1*$^{-/-}$ lungs collected and acid-fast stained at the same time as those of controls. Magnifications (×100) of select areas (i to iii) showed AFB localizing near the lung vasculature (i), near the airways (iia and b), and in or on alveolar pneumocytes (iii); images in frames iia and iib are serial sections of the same area used to help resolve the morphology of the cell containing AFB. Vs, vessel; Br, bronchiole; Al, alveoli.

higher in the lungs of *il12rb1*$^{-/-}$ mice than in wild-type controls (Fig. 1A). Following the dissemination of *M. tuberculosis* from the lungs (an event that occurs approximately 10 days postinfection in wild-type animals [52]), bacterial growth continued to remain unhindered in both the spleen and liver of *il12rb1*$^{-/-}$ mice (Fig. 1B and C). Collectively, these results demonstrate that *il12rb1*$^{-/-}$ mice are similar to *IL12RB1* null individuals in their susceptibility to mycobacterial infection as measured by *M. tuberculosis* burden.

Granulomatous accumulations in *il12rb1*$^{-/-}$ mice are abnormal and associate with decreased transcription of *ifng* and *nos2*. Like individuals with functional *IL12RB1* alleles, *IL12RB1* null individuals develop granulomas in response to mycobacterial infection (4, 16). The composition of and number of AFB in these granulomas, however, are different than those of granulomas in individuals with intact *IL12RB1* alleles (4, 16). As an additional measure of TB susceptibility in *il12rb1*$^{-/-}$ mice, therefore, we assessed the extent of pulmonary pathology in *il12rb1*$^{-/-}$ mice

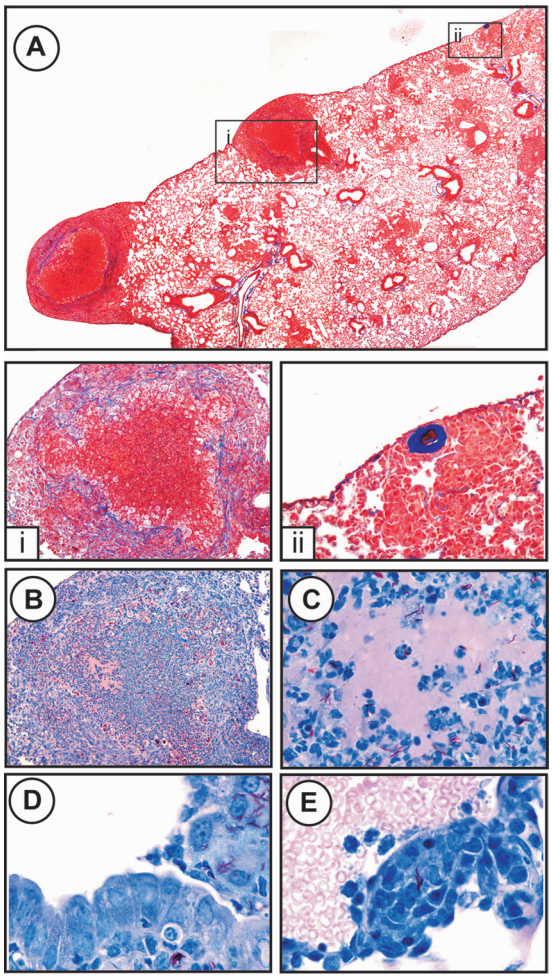

FIG 3 Granulomatous accumulations in *il12rb1*$^{-/-}$ mice are distinct from those found in wild-type mice. Fifty days following aerogenic infection with *M. tuberculosis*, lung sections from C57BL/6 and *il12rb1*$^{-/-}$ mice were stained with Masson's trichrome in order to visually assess the degree of pulmonary pathology. Shown are representative micrographs of features observed in *il12rb1*$^{-/-}$ mice that were not present in C57BL/6 controls. (A) Micrograph at a ×4 magnification of an *il12rb1*$^{-/-}$ lung at day 50 postinfection showing the presence of two densely red staining regions, one of which is shown at ×10 magnification in the inset below (i). Shown in inset ii is a ×40 magnification of a pulmonary ossification found in the same *il12rb1*$^{-/-}$ lung. (B) An acid-fast stain of a serial section located adjacent to the trichrome-stained region shown in panel Ai was used to visualize the localization of AFB relative to the collagenous (i.e., blue) perimeter seen in panel Ai. (C to E) Micrographs at ×100 magnification of select features observed in panel B, namely, the presence of AFB in the necrotic center (C), AFB on or near bronchial epithelium (D), and AFB near the vascular epithelium (E).

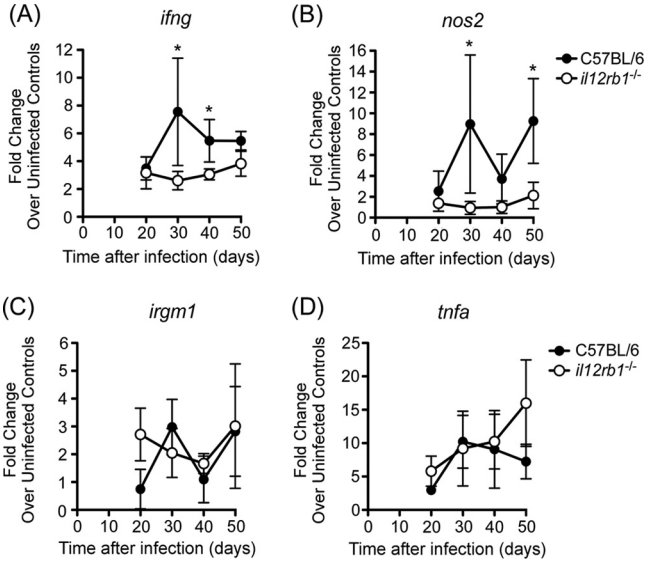

FIG 4 *M. tuberculosis*-induced expression of host-protective *ifng* and *nos2* is lower in *il12rb1*$^{-/-}$ mice. mRNA from the lungs of *M. tuberculosis*-infected C57BL/6 and *il12rb1*$^{-/-}$ mice was collected at select times postinfection; subsequently generated cDNA was used for real-time quantitation of *ifng* (A), *nos2* (B), *irgm1* (C), and *tnfa* (D) expression levels. Expression of each gene was normalized to that of *gapdh* in the same sample; data were analyzed via $\Delta\Delta C_T$ analysis (7) and is expressed as fold expression over the levels found in genotype-matched uninfected controls. Each data point represents the mean ± SD of the values at each time point and show one experiment representative of a total of three. For the difference between values of *il12rb1*$^{-/-}$ relative to C57BL/6 mice, $P \leq 0.05$ (*) by Student's *t* test.

and compared it to that observed in wild-type controls (19, 37). While it is widely recognized that *M. tuberculosis*-infected mice do not develop classical granulomas (6), pulmonary leukocyte accumulations do, nevertheless, develop in mice that comprise many of the same lineages and proinflammatory cytokines found in human granulomas (55).

In wild-type mice, granulomatous accumulations developed over the first 50 days of infection in a manner identical to that previously described (55) (data not shown). In *il12rb1*$^{-/-}$ mice, however, these accumulations were characterized by several features not observed in wild-type controls (Fig. 3). Specifically, accumulations in *il12rb1*$^{-/-}$ mice contained necrotic centers (Fig. 3Ai and C) and abundant numbers of AFB (Fig. 3B, primarily found near a collagenous perimeter of the necrotic foci) as well as occasional pulmonary ossifications (Fig. 3Aii). As was also observed at day 20 postinfection (Fig. 2Bi to iii), AFB in *il12rb1*$^{-/-}$ mice could be seen directly associating with or near bronchial epithelia (Fig. 3D) and vascular endothelia (Fig. 3E). Regarding the expression of host-protective genes in these same lungs, beginning at day 30 postinfection, fold increase in the mRNA levels of host-protective *ifng* and *nos2* were all lower in *il12rb1*$^{-/-}$ lungs than in those of wild-type controls (Fig. 4A and B). Notably, mRNA levels of *irgm1* were unaffected by *il12rb1* deficiency (Fig. 4C), and levels of *tnfa* mRNA were increased compared to those expressed in wild-type animals at days 40 and 50 postinfection (Fig. 4D). These data, when combined with that of bacterial burden (Fig. 1), collectively demonstrate that *il12rb1* is required to both control pulmonary *M. tuberculosis* infection and regulate the development of pulmonary pathology. Furthermore, given the similar disease characteristics in *il12rb1*$^{-/-}$ mice and *IL12RB1* null individuals, we also conclude that the mouse model is suitable for testing which lineage(s) must express *IL12RB1* for tubercular control to occur.

***il12rb1* expression by *rag1*-dependent lineages is required to control *M. tuberculosis* infection.** The functions of *rag1*-dependent lineages are compromised in the absence of *IL12RB1* (14, 36). Whether *il12rb1* expression by *rag1*-dependent lineages is required to control *M. tuberculosis* infection, however, has never been formally tested. To do this, we generated radiation bone marrow chimeras in which *il12rb1* deficiency was restricted to

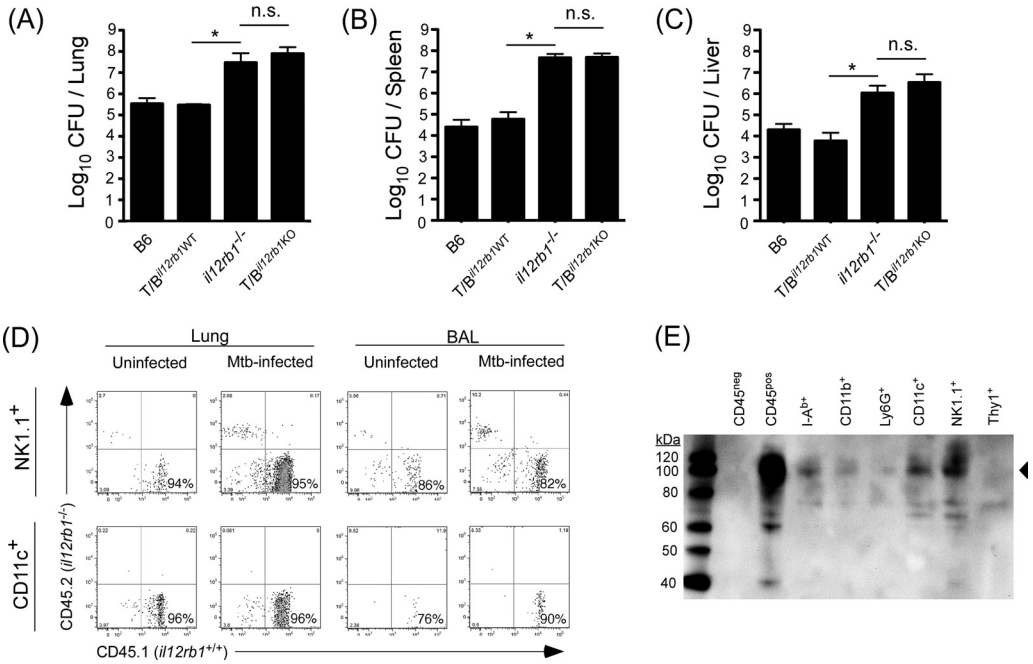

FIG 5 *il12rb1* expression by *rag1*-dependent lineages is required to control *M. tuberculosis* infection. Lethally irradiated $rag1^{-/-}$ mice were reconstituted with one of either of the following bone marrow preparations: 100% C57BL/6, 80% $rag1^{-/-}$ and 20% $il12rb1^{+/+}$ cells (T/B^{il12rb1WT} mice), 100% $il12rb1^{-/-}$, or 80% $rag1^{-/-}$ and 20% $il12rb1^{-/-}$ (T/B^{il12rb1KO} mice) cells. All chimeras were simultaneously infected via aerosol with *M. tuberculosis* H37Rv. Fifty days postinfection with *M. tuberculosis*, bacterial burdens in the lungs (A), spleen (B), and liver (C) were determined. Each bar represents the mean + SD of the values observed and show one experiment representative of a total of three. *, $P \leq 0.05$, between the values of two groups as determined by ANOVA; ns, not significant. (D and E) To confirm that innate lineages retained *il12rb1* expression in T/B^{il12rb1KO} mice, CD45.1 congenic mice were used as $il12rb1^{+/+}$ donors so as to determine, via flow cytometry of both lung and BAL cell preparations, the percentage of NK1.1$^+$ (D, top row) and CD11c$^+$ (D, bottom row) lineages that were *il12rb1* sufficient (CD45.1$^+$) or *il12rb1* deficient (CD45.2$^+$). (E) These same lineages (i.e., NK1.1$^+$ and CD11c$^+$), as well as CD45^{neg}, CD45^{pos}, I-Ab$^+$, CD11b$^+$, Ly6G$^+$, and Thy1$^+$ cells from *M. tuberculosis*-infected T/B^{il12rb1KO} mice, were magnetically purified and subjected to denaturing SDS-PAGE and Western analysis to visualize IL-12Rβ1 protein expression. Blots were probed with polyclonal anti-mouse IL-12Rβ1; the location of IL-12Rβ1 protein is indicated by an arrow (right) and is consistent with a 100- to 120-kDa glycosylated product as judged by size standards (left).

rag1-dependent lineages (i.e., T and B cells). Specifically, lethally irradiated $rag1^{-/-}$ mice were reconstituted with a bone marrow admixture comprising 80% $rag1^{-/-}$ and 20% $il12rb1^{-/-}$ cells; any *rag1*-dependent lineages in the resultant chimera must, by definition, be *il12rb1* deficient, while the majority of *rag1*-independent lineages (e.g., NK cells) retain intact *il12rb1* alleles. These chimeras, with $il12rb1^{-/-}$ T/B cells, are hereinafter referred to as T/B^{il12rb1KO} mice. For controls, we used lethally irradiated $rag1^{-/-}$ mice reconstituted with either 100% C57BL/6 bone marrow, 100% $il12rb1^{-/-}$ bone marrow, or a bone marrow admixture comprising 80% $rag1^{-/-}$ and 20% $il12rb1^{+/+}$ cells (T/B^{il12rb1WT} mice). For generating all chimeras, $rag1^{-/-}$ mice were used as hosts to eliminate any potential complicating effects of radioresistant T/B cells (8); the efficiency of host bone marrow replacement using our protocols was ≥94% as tested using CD45.1 congenic bone marrow (Fig. 5D).

Using bacterial burden as our primary readout, we observed at 50 days postinfection that T/B^{il12rb1KO} mice exhibited lung burdens that were both significantly higher than those observed in T/B^{il12rb1WT} mice and equal to those levels found in $il12rb1^{-/-}$ mice (Fig. 5A). In the spleen and liver, bacterial burdens in T/B^{il12rb1KO} mice were also above those of T/B^{il12rb1WT} controls and equal to those observed in $il12rb1^{-/-}$ mice (Fig. 5B and C). In all organs examined, control T/B^{il12rb1WT} mice exhibited bacterial burden levels equal to those of wild-type animals (Fig. 5A to C). Using CD45.1 congenic mice as $il12rb1^{+/+}$ donors, we confirmed that the majority of both NK1.1$^+$ and CD11c$^+$ lineages in T/B^{il12rb1KO} mice were *il12rb1* sufficient (Fig. 5D); Western analysis of magnetically sorted lineages also confirmed that innate I-A^{b+}, CD11b$^+$, Ly6G$^+$, CD11c$^+$, and NK1.1$^+$ lineages of infected T/B^{il12rb1KO} mice expressed IL-12Rβ1 protein (Fig. 5E). As anticipated, Thy1$^+$ cells in the same T/B^{il12rb1KO} mice did not express IL-12Rβ1; supporting a role for hematopoietic *il12rb1* expression, the CD45^{neg} fraction of *M. tuberculosis*-infected lungs did not express IL-12Rβ1 protein (Fig. 5E). From these data, we conclude that *il12rb1* expression by *rag1*-dependent lineages is required to control *M. tuberculosis* infection and that restriction of *il12rb1* deficiency solely to *rag1*-dependent lineages allows for the full transfer of the $il12rb1^{-/-}$ phenotype.

***ifng* expression by *rag1*-dependent lineages contributes to control of *M. tuberculosis* infection.** A well-known consequence of IL-12 signaling in hematopoietic lineages is production of IFN-γ. IFN-γ is essential for control of experimental TB (12, 22) and, as demonstrated by flow cytometric analysis of Yeti mouse lungs (64), is solely produced by hematopoietic cells following *M. tuberculosis* infection (Fig. 6A and B), including CD4$^+$ T cells, CD8$^+$ T cells, NK1.1$^+$ cells, and GR1$^+$ granulocytes (Fig. 6C and D). The contribution of each lineage to the total IFN-γ response changes over the course of infection (Fig. 6D). Of particular note is the decline in NK cell representation following *M. tuberculosis* infection and the concomitant increase in representation of CD4$^+$, CD8$^+$, and GR1$^+$ cells (Fig. 6D). That most NK cells con-

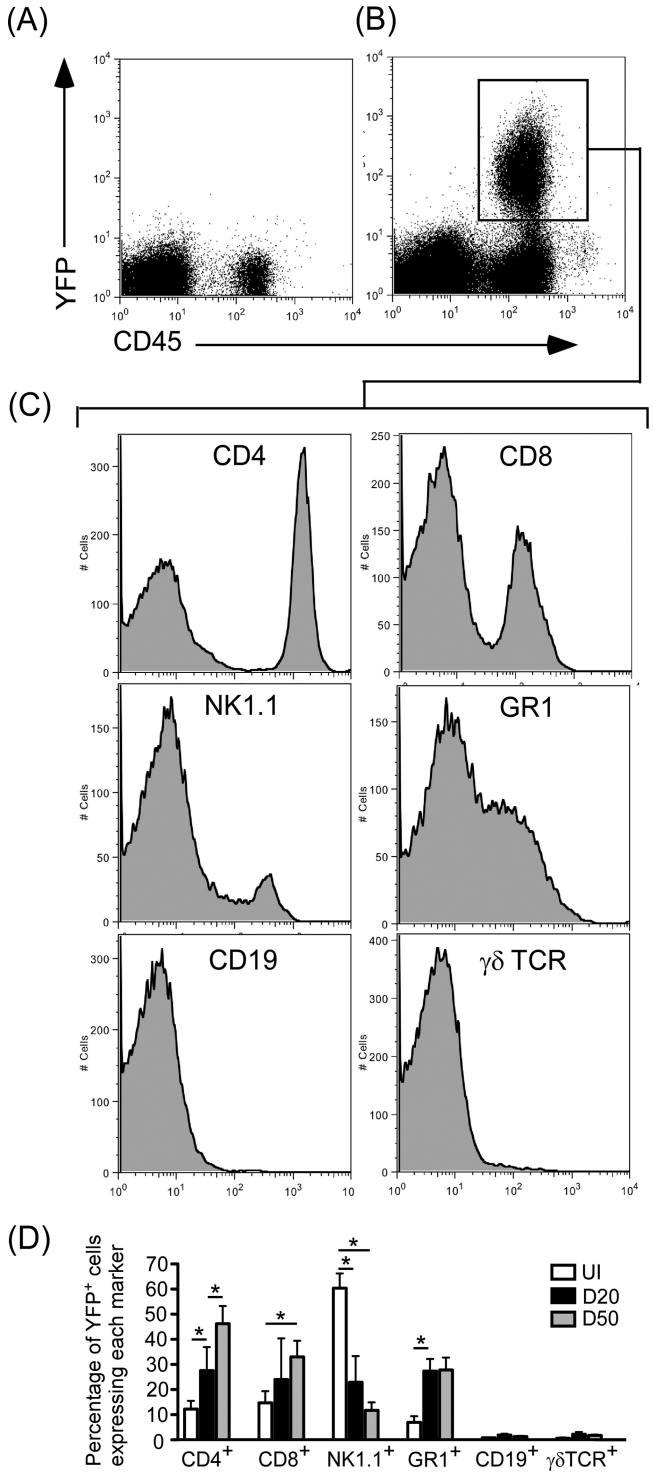

FIG 6 *ifng* is expressed by multiple hematopoietic subsets during experimental TB. C57BL/6 and IFN-γ–eYFP reporter mice (i.e., Yeti mice) (54) were infected via aerosol with *M. tuberculosis*. At 50 days postinfection, lung cell preparations were stained with a panel of antibodies for FACS determination of which cells were expressing *ifng* at that point in time. Using a gating strategy based on their forward scatter and side scatter characteristics, CD45-stained C57BL/6 cells served as a negative control for YFP fluorescence (A) while Yeti cells demonstrated all YFP signal to be found among $CD45^+$ cells (B). (C) Among $CD45^+$ YFP^+ cells, we surveyed the extent to which $CD4^+$, $CD8^+$, $NK1.1^+$, $GR1^+$, $CD19^+$, or γδ-TCR^+ events were present. Shown are representative histograms for each subset. Shown are data from one experiment that is representative of a total of two (four mice per experiment). (D) Cumulative data demonstrating the percentage of $CD45^+$ YFP^+ cells expressing either of the following lineage markers at indicated times following infection: CD4, CD8, NK1.1, GR1, CD19, or γδ-TCR. Data are combined from two separate experiments, with four mice per time point per experiment; bars represent the mean percentage of YFP^+ events expressing each marker ± SD. A significant difference ($P \leq 0.05$) between two time points (for a given lineage) is indicated by an asterisk. D20, day 20 postinfection; D50, day 50 postinfection; UI, uninfected.

stitutively express IFN-γ mRNA at homeostasis has been previously observed (64). Absent among IFN-γ^+ events in the *M. tuberculosis*-infected lung are $CD45^{neg}$ cells (Fig. 6B); $CD19^+$ cells and γδ-T cells are also minimal among IFN-γ^+ cells (Fig. 6C and D). Furthermore, and consistent with the well-established need for IL-12 in promoting T-cell IFN-γ responses to other intracellular infections (26, 28), the percentage of $Thy1^+$ IFN-γ^+ cells following *M. tuberculosis* infection is reduced in the absence of *il12rb1* (Fig. 7A to C). Confirming the essential role of hematopoietic *ifng* expression, reconstitution of lethally irradiated $rag1^{-/-}$ mice with $ifng^{-/-}$ bone marrow completely transfers the $ifng^{-/-}$ phenotype (Fig. 8A); these data rule out the possibility that nonhematopoietic lineages are a source of protective IFN-γ.

Recently, the significance of T-cell IFN-γ expression as it pertains to *M. tuberculosis* control was brought into question by the results of Gallegos et al. and Torrado and Cooper (24, 70), who demonstrated that *ex vivo* differentiated $ifng^{-/-}$ T cells controlled aerogenic *M. tuberculosis* infection just as well as $ifng^{+/+}$ T cells in the first 21 days of infection. In the low-dose aerogenic model of TB, however, ~20 days postinfection is the very earliest point at which all IFN-γ-producing T cells have arrived into the lungs of *M. tuberculosis*-infected animals (31, 53). More importantly, significant differences between wild-type and T-cell-deficient (or even *ifngr*-deficient) mice have historically not been observed until after the 20-day time point (Fig. 8A) (17, 41). To resolve this issue and directly test whether IFN-γ expression by *rag1*-dependent lineages was required to control primary *M. tuberculosis* infection, we generated (in a manner analogous to that described above) radiation bone marrow chimeras comprising $rag1^{-/-}$ hosts reconstituted with a bone marrow admixture of either 80% $rag1^{-/-}$ and 20% $ifng^{-/-}$ cells (T/B^{ifngKO} mice) or 80% $rag1^{-/-}$ and 20% $ifng^{+/+}$ cells (T/B^{ifngWT} mice). As is shown in Fig. 8A, at 20 days postinfection, lung bacterial burdens in T/B^{ifngKO} and T/B^{ifngWT} mice were equal. By 40 days postinfection, however, T/B^{ifngKO} mice exhibited burdens in the lung that were significantly higher than those of T/B^{ifngWT} controls (Fig. 8A). A similar pattern was observed in the spleen and liver following *M. tuberculosis* dissemination to these organs, with T/B^{ifngKO} mice exhibiting burdens in the spleen (Fig. 8B) and liver (Fig. 8C) that were significantly higher than those of T/B^{ifngWT} controls beginning 30 days postinfection. Despite being higher than T/B^{ifngWT} controls, however, bacterial burdens in T/B^{ifngKO} mice were significantly less than those in complete (100%) $ifng^{-/-}$ mice in all organs tested (Fig. 8A to C). The gross visible abnormalities associated with *M. tuberculosis*-infected $ifng^{-/-}$ lungs (22) were also not observed in T/B^{ifngKO} mice (data not shown). Collectively, these data demonstrate that *ifng* expression by *rag1*-dependent lineages contributes to tubercular control; however, the absence of *ifng* in *rag1*-dependent lineages does not completely account for the phenotype of $ifng^{-/-}$ mice.

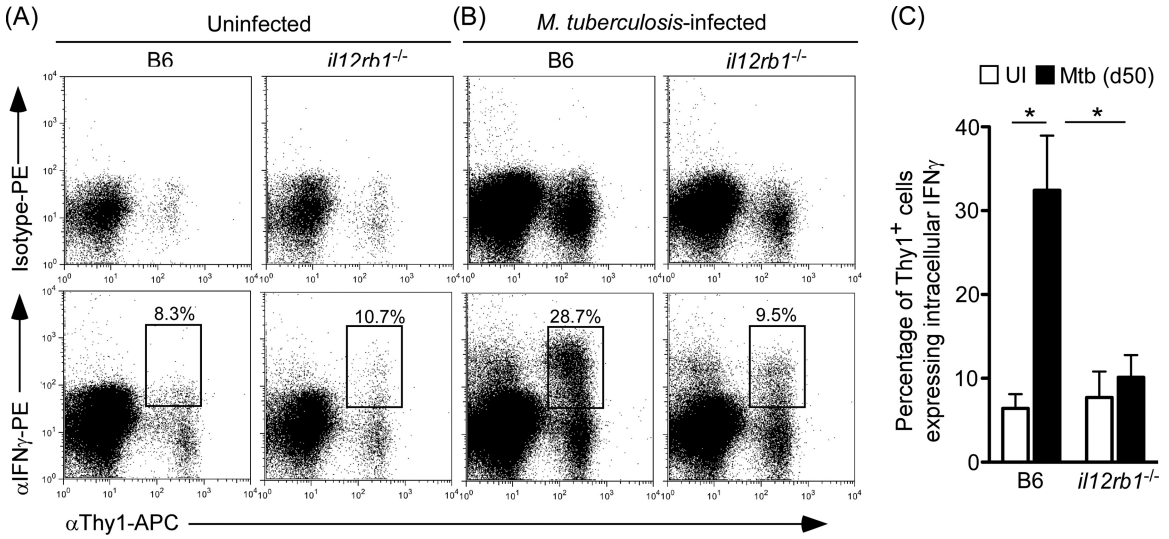

FIG 7 *il12rb1* positively regulates T cell *ifng* expression following *M. tuberculosis* infection. Lung cell preparations from C57BL/6 and *il12rb1*$^{-/-}$ mice that were either uninfected (A) or *M. tuberculosis* infected (50 days postinfection) (B) were stained for T-cell marker Thy1 and intracellular IFN-γ. Isotype control staining (i.e., the top row) was used to discriminate positive staining for IFN-γ. Shown are representative FACS dot plots from each condition; inside the plots of αIFN-γ-stained cells (i.e., the bottom row) are box gates indicating the percentage of Thy1^{+} cells positive for IFN-γ. (C) Cumulative data demonstrating the percentage of Thy1^{+} cells expressing IFN-γ, as determined by intracellular cytokine staining, in both C57BL/6 and *il12rb1*$^{-/-}$ lungs after 50 days of *M. tuberculosis* infection (Mtb; solid bars). Data from uninfected (UI) lungs (open bars) are also shown. Data are combined from three separate experiments, with four mice per time point per experiment; bars represent the mean percentage ± SD. A significant difference ($P \leq 0.05$) between uninfected and infected animals is indicated by an asterisk.

***il12rb1*$^{+/+}$ T cells are dominant over *il12rb1*$^{-/-}$ T cells during *M. tuberculosis* infection.** Given the importance of T-cell *ifng* expression to *M. tuberculosis* control (Fig. 8), we wished to determine the relative dominance of *il12rb1*$^{+/+}$ T cells versus *il12rb1*$^{-/-}$ T cells as it pertains to production of IFN-γ. In other words, when *il12rb1*$^{+/+}$ and *il12rb1*$^{-/-}$ T cells coexist within the same infection, does the presence of *il12rb1*$^{+/+}$ T cells influence the expression of IFN-γ by *il12rb1*$^{-/-}$ T cells, and vice versa? To

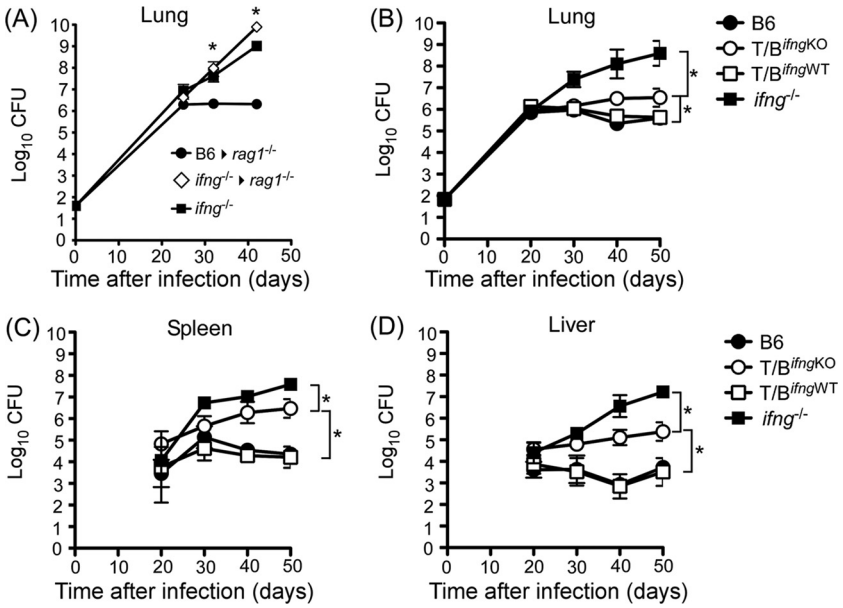

FIG 8 *ifng* expression by *rag1*-dependent lineages contributes to *M. tuberculosis* control. (A) Lethally irradiated *rag1*$^{-/-}$ mice were reconstituted with either 100% C57BL/6 or 100% *ifng*$^{-/-}$ bone marrow; 4 weeks later, these chimeras were aerosol infected with *M. tuberculosis* H37Rv alongside *ifng*$^{-/-}$ controls. At select times postinfection, lung *M. tuberculosis* burdens were determined. *, statistically significant difference from C57BL/6 or *rag1*$^{-/-}$ controls. (B to D) Lethally irradiated *rag1*$^{-/-}$ mice were reconstituted with one of either of the following bone marrow preparations: 100% C57BL/6, 80% *rag1*$^{-/-}$ and 20% *ifng*$^{+/+}$ cells (T/B^{ifngWT} mice), or 80% *rag1*$^{-/-}$ and 20% *ifng*$^{-/-}$ (T/B^{ifngKO} mice). All chimeras were simultaneously infected via aerosol with *M. tuberculosis* H37Rv. At indicated times following infection, *M. tuberculosis* burdens in the lungs (B), spleen (C), and liver (D) were determined. Each data point in panels A to D represents the mean ± SD of the values observed, and panels show one experiment representative of a total of two. *, $P \leq 0.05$, between indicated groups as determined by ANOVA of all data points collected at that particular time.

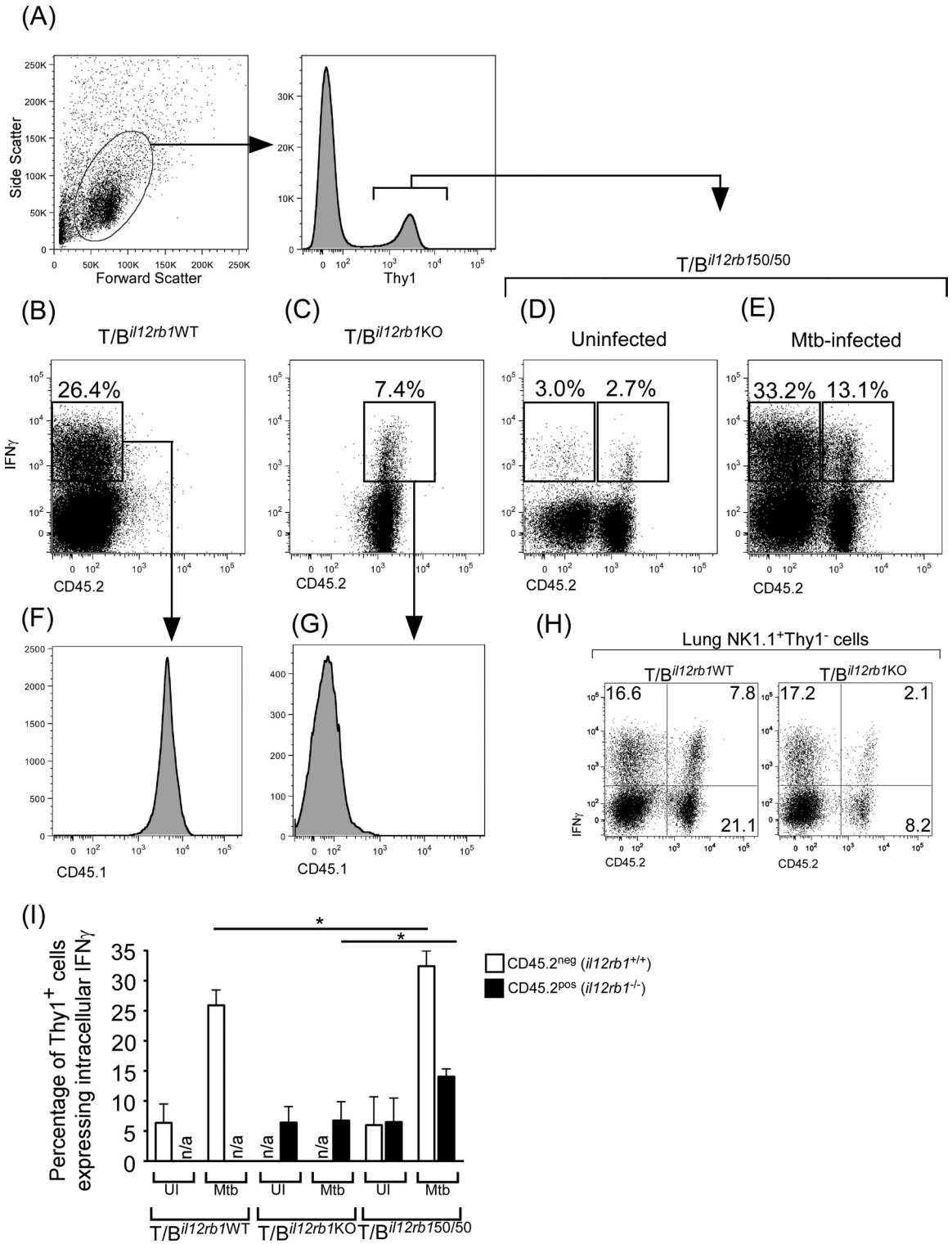

FIG 9 *il12rb1*$^{+/+}$ T cells exhibit dominance over *il12rb1*$^{-/-}$ T cells during *M. tuberculosis* infection. Lethally irradiated *rag1*$^{-/-}$ mice were reconstituted with one of either of the following bone marrow preparations: 80% *rag1*$^{-/-}$ and 20% CD45.1.*il12rb1*$^{+/+}$ (T/B^{il12rb1WT}), 80% *rag1*$^{-/-}$ and 20% *il12rb1*$^{-/-}$ (T/B^{il12rb1KO}), or 80% *rag1*$^{-/-}$, 10% CD45.1.*il12rb1*$^{+/+}$, and 10% *il12rb1*$^{-/-}$ (T/B$^{il12rb150/50}$) cells. Following *M. tuberculosis* infection, we determined the relative percentage of IFN-γ^{+} cells among cells of either the *il12rb1*$^{+/+}$ (i.e., CD45.1^{pos}) or *il12rb1*$^{-/-}$ (i.e., CD45.1^{neg}) genotype at day 50 postinfection. Shown in panel A is our gating strategy for identification of T lymphocytes. Examination of lung T lymphocytes in *M. tuberculosis*-infected T/B^{il12rb1WT} (B) and T/B^{il12rb1KO} (C) mice established the percentages of T cells expressing IFN-γ in the absence of T cells of a different genotype, whether they be CD45.2^{neg} CD45.1^{pos} *il12rb1*$^{+/+}$ cells (F) or CD45.2^{pos} CD45.1^{neg} *il12rb1*$^{-/-}$ cells (G). (D and E) The same analysis was extended to T/B$^{il12rb150/50}$ mice that had been either left uninfected (D) or *M. tuberculosis* infected (E) at the same time as the controls shown in panels B and C. Box gates in panels B to E indicate the percentages of IFN-γ^{+} events among T cells of each genotype. (H) IFN-γ expression by lung NK cells 30 days after *M. tuberculosis* infection in both T/B^{il12rb1WT} (left) and T/B^{il12rb1KO} (right) chimeric

test this, we generated and infected radiation bone marrow chimeras in which half of all T/B-cell lineages were *il12rb1*$^{+/+}$ and half were *il12rb1*$^{-/-}$ (hereinafter here referred to as T/B$^{il12rb150/50}$ mice). Specifically, irradiated *rag1*$^{-/-}$ hosts were reconstituted with an admixture of 80% *rag1*$^{-/-}$, 10% CD45.1.*il12rb1*$^{+/+}$, and 10% *il12rb1*$^{-/-}$ bone marrow. These chimeric T/B$^{il12rb150/50}$ mice were simultaneously generated alongside control chimeras comprising *rag1*$^{-/-}$ mice reconstituted with either 80% *rag1*$^{-/-}$ and 20% CD45.1*il12rb1*$^{+/+}$ (T/B^{il12rb1WT}) or 80% rag1$^{-/-}$ and 20% *il12rb1*$^{-/-}$ (T/B^{il12rb1KO}) bone marrow.

Consistent with the phenotype of T cells of nonchimeric *il12rb1*$^{-/-}$ and *il12rb1*$^{+/+}$ mice (Fig. 7), at 50 days postinfection T/B^{il12rb1KO} mice produced fewer IFN-γ^{+} T cells than T/B^{il12rb1WT} controls (Fig. 9A to C). Staining for CD45.2 and CD45.1 allowed for FACS discrimination of T cells of either the *il12rb1*$^{+/+}$ (Fig. 9F) or *il12rb1*$^{-/-}$ (Fig. 9G) genotype, respectively. IFN-γ expression levels by *il12rb1*$^{+/+}$ NK cells in both T/B^{il12rb1WT} and T/B^{il12rb1KO} mice were comparable (Fig. 9H); NK cells derived from *il12rb1*$^{-/-}$ bone marrow comprised approximately 10% of total lung NK cells (Fig. 9H, right). When this analysis was extended to T/B$^{il12rb150/50}$ mice, we observed that, compared to their counterparts in T/B^{il12rb1KO} mice, the percentage of IFN-γ^{+} *il12rb1*$^{-/-}$ T cells increased in the presence of *il12rb1*$^{+/+}$ T cells (Fig. 9E and I). Unexpectedly, we also observed that *il12rb1*$^{+/+}$ T cells modestly increased their own production of IFN-γ when *il12rb1*$^{-/-}$ T cells were present (Fig. 9E and I). Both *il12rb1*$^{+/+}$ and *il12rb1*$^{-/-}$ T cells increased their expression levels of IFN-γ over their counterparts in uninfected T/B$^{il12rb150/50}$ controls (Fig. 9D and I). We conclude from this analysis that *il12rb1*$^{+/+}$ T cells exhibit dominance over *il12rb1*$^{-/-}$ T cells during *M. tuberculosis* infection by both promoting IFN-γ production by *il12rb1*$^{-/-}$ T cells and enhancing their own production of this significant cytokine.

***il12rb1*$^{-/-}$ T cells exhibit decreased proliferative capacity and altered polarization following *M. tuberculosis* infection.** Since impaired T-cell expression of IFN-γ did not fully account for the phenotypic differences between T/B^{il12rb1KO} and T/B^{il12rb1WT} mice, we determined, via flow cytometry, whether other phenotypic differences (beyond IFN-γ) existed between *il12rb1*$^{-/-}$ and *il12rb1*$^{+/+}$ T cells. Specifically, we infected T/B$^{il12rb150/50}$ mice and, at day 50 postinfection, assessed proliferative capacity (via BrdU incorporation), activation status (CD44), expression of the master transcription factors Tbet and Foxp3, and intracellular levels of effector cytokines TNF-α and IL-17. As before (Fig. 9), using CD45 congenic mice as *il12rb1*$^{+/+}$ donors afforded the ability to directly compare *il12rb1*$^{-/-}$ (CD45.2-positive [CD45.2^{pos}]) and *il12rb1*$^{+/+}$ (CD45.2^{neg}) T cells within the same infected mouse. Both CD4^{+} (Fig. 10A to F) and CD8^{+} (Fig. 10G to L) T cells were examined in this manner. Regarding CD4^{+} T cells, despite being activated to a similar degree (Fig. 10A), CD45.2^{neg} cells displayed a greater proliferative capacity than CD45.2^{pos} cells (Fig. 10B). The polarization of CD45.2^{pos} cells was also altered relative to CD45.2^{neg} cells, with CD45.2^{pos} cells expressing lower levels of T_H1-associated proteins Tbet (Fig. 10C) and tumor necrosis factor alpha (TNF-α) (Fig. 10E), and increased levels of regulatory T cell (T_{Reg})-associated transcription factor Foxp3 (Fig. 10D). Levels of proinflammatory IL-17 were similarly low in CD4^{+} T cells of either genotype (Fig. 10F). Regarding CD8^{+} T cells, CD45.2^{neg} and CD45.2^{pos} cells expressed similar levels of CD44 (Fig. 10G). However, despite the appearance of a more discrete CD45.2^{+} BrdU^{+} subset (Fig. 10H), *il12rb1*$^{-/-}$ CD8^{+} cells displayed a lower proliferative potential relative to their *il12rb1*$^{+/+}$ counterparts when the data are expressed as the percentage of CD8^{+} cells taking up BrdU (Fig. 10H). CD8 expression of Tbet (67) and TNF-α was also lower among CD45.2^{pos} cells (Fig. 10I and K); Foxp3 and IL-17 expression levels were equally low in CD45^{neg} and CD45^{pos} cells (Fig. 10J and L). The cumulative data from both CD4^{+} and CD8^{+} T cells are shown in Fig. 10M to N. Collectively, these data demonstrate that both CD4^{+} and CD8^{+} *il12rb1*$^{-/-}$ T cells exhibit decreased proliferative capacities and altered polarization following *M. tuberculosis* infection.

DISCUSSION

IL-12 family members [IL-12, IL-23, and IL-12(p40)$_2$] directly and indirectly influence the function of nearly all hematopoietic cell types, including those derived from myeloid progenitors (erythrocytes [42, 43], thrombocytes [9], mast cells [75], basophils [60], neutrophils [44], eosinophils [40], macrophages [58], and dendritic cells [33]) as well as lymphoid progenitors (NK-cells ([25], NK T cells [73], B cells [39], γδ-T cells [71], CD4^{+} αβ-T cells [68], and CD8^{+} αβ-T cells [20, 49]). The effects of IL-12 family members on nonhematopoietic lineages are less known although bronchial epithelial cells have been demonstrated to express the receptor for IL-12 (1). The activity of each IL-12 family member is dependent on the products of *IL12RB1*, a gene that in both humans and mice (*il12rb1*) expresses multiple mRNA isoforms, including the type I integral membrane protein IL-12Rβ1. IL-12Rβ1 serves as a low-affinity receptor for the p40 subunit of each IL-12 family member (11, 51). The extracellular portion of IL-12Rβ1 contains the cytokine-binding region essential for physical association with IL-12 or IL-23, while the cytoplasmic portion acts in concert with IL-12Rβ2/IL-23R to transmit intracellular signals via preassociated Janus kinases TYK2 and JAK2. Transcription of *IL12RB1* is increased during active tuberculosis in humans (69) and is critical for the control of both tuberculous and nontuberculous forms of mycobacterial disease (3, 16).

Here, we have demonstrated that in the early stages of experimental tuberculosis, *il12rb1* functions primarily through *rag1*-dependent lineages to control mycobacterial growth and limit pul-

mice. Dot plots are gated off NK1.1^{+} Thy1^{-} cells, with numbers indicating the relative percentages of intracellular IFN-γ^{+} NK cells with either an *il12rb1*$^{+/+}$ or *il12rb1*$^{-/-}$ genotype. CD45.1 congenic mice were used as *il12rb1*$^{+/+}$ donors so as to distinguish between NK cells of either genotype. In T/B^{il12rb1WT} mice (left), both CD45.2^{+} and CD45.2^{-} cells are *il12rb1*$^{+/+}$; in T/B^{il12rb1KO} mice (right), by definition, CD45.2^{+} cells are *il12rb1*$^{-/-}$, and CD45.2^{-} cells are *il12rb1*$^{+/+}$. All dot plots are representative of two separate experiments with four mice per group per experiment. (I) Cumulative data (the experiments performed for panels A to G) demonstrating the percentage of lung CD45.2^{neg} (i.e., *il12rb1*$^{+/+}$) and CD45.2^{pos} (i.e., *il12rb1*$^{-/-}$) Thy1^{+} cells expressing intracellular IFN-γ in either of the following groups of chimeras: T/B^{il12rb1WT}, T/B^{il12rb1KO}, and T/B$^{il12rb150/50}$ mice. Data from both uninfected (UI) and *M. tuberculosis*-infected (day 50) mice are shown; bars represent the mean ± SD of the percentages observed and are the combined data from eight mice per group (two separate aerosol experiments with four mice/group/time point). A statistically significant difference ($P \leq 0.05$) between two groups is indicated with an asterisk and was determined by ANOVA of all data points.

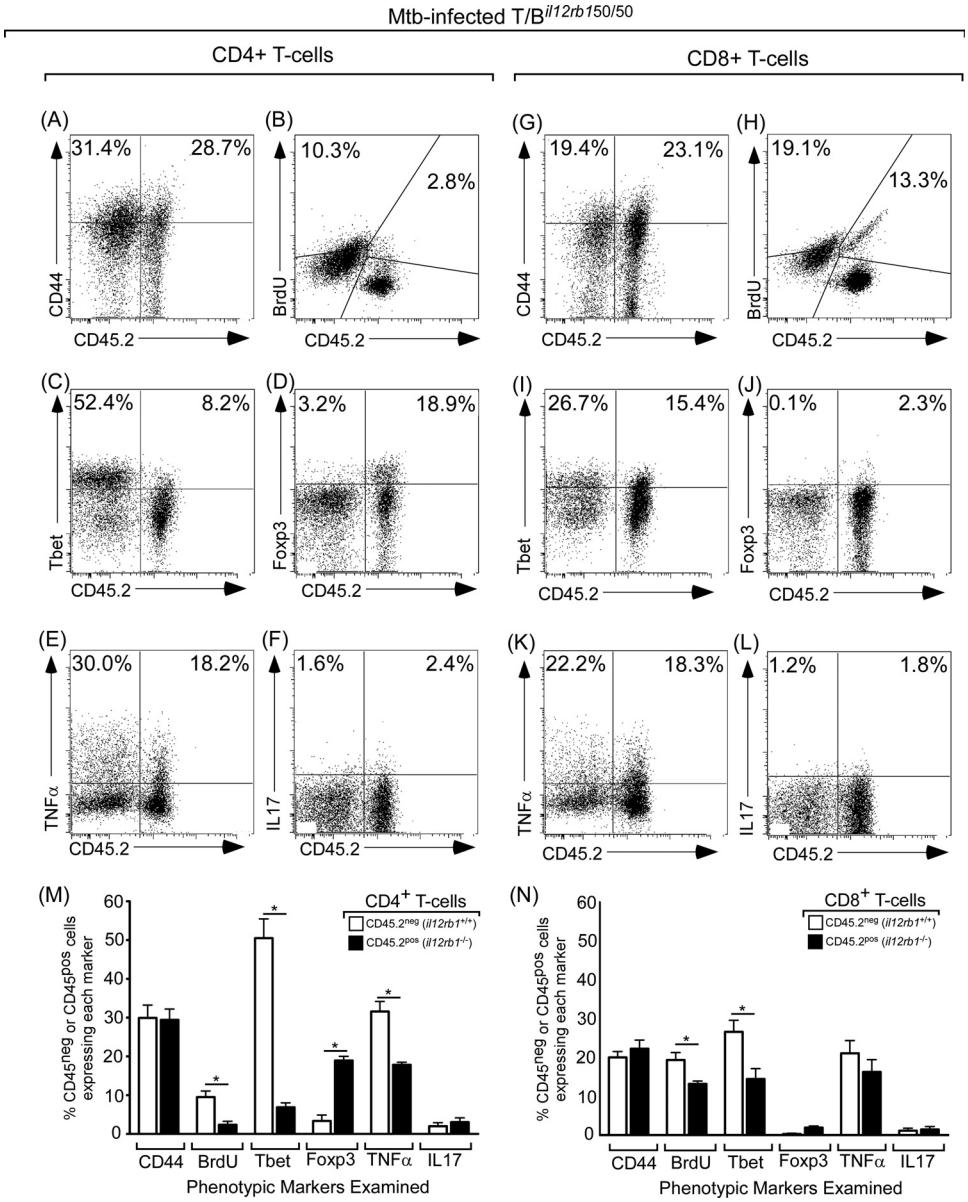

FIG 10 *il12rb1*$^{-/-}$ T cells display defective proliferative capacity and aberrant polarization. T/B$^{il12rb150/50}$ mice were infected via aerosol with ~80 CFU of virulent H37Rv. At 48 days after infection, mice were treated i.p. with BrdU containing saline; 2 days later (day 50 of infection), lung cell preparations were stained with anti-BrdU antibodies as well as the indicated extracellular (i.e., CD4, CD8, and CD44) and intracellular (Tbet, Foxp3, TNF-α, and IL-17) markers of T cell differentiation. Costaining for CD45.2 was used to discriminate between *il12rb1*$^{+/+}$ (i.e., CD45.2^{neg}) and *il12rb1*$^{-/-}$ (i.e., CD45.2^{pos}) populations; shown are representative dot plots of both CD4$^+$ (A to F) and CD8$^+$ (G to L) lung cells. For each dot plot, the numbers in the upper left and right quadrants indicate, respectively, the percentages of *il12rb1*$^{+/+}$ and *il12rb1*$^{-/-}$ T cells expressing either CD44 (A and G), incorporated BrdU (B and H), Tbet (C and I), Foxp3 (D and J), TNF-α (E and K), or IL-17 (F and L). (M and N) Cumulative CD4$^+$ and CD8$^+$ T cell expression data of the indicated markers from two experiments with four T/B$^{il12rb150/50}$ mice per experiment. Each bar represents the mean percentage observed ± SD; a statistically significant difference ($P \leq 0.05$) between two groups is indicated with an asterisk and was determined by a Student's *t* test of all data points for an individual marker.

monary pathology. This *rag1*-dependent lineage likely represents αβ-T cells, given the extensive analysis of North et al., who demonstrated the essential role αβ-T cells have in containing bacteria during this phase of experimental TB (41, 45, 46) and the similarly nonessential role of γδ-T cells (41), NK T cells (5, 18, 66), and B cells (30) in the same mouse model. *il12rb1*$^{-/-}$ T cells have a decreased capacity to express protective *ifng*, which partially accounts for the elevated bacterial burdens in T/B^{il12rb1KO} mice. *il12rb1*$^{+/+}$ T cells exhibit dominance over *il12rb1*$^{-/-}$ T cells by promoting the expression of IFN-γ in the latter population. This is likely due to an ability of *il12rb1*$^{+/+}$-derived IFN-γ to promote its own transcription in an IL-12-independent manner. Unexpectedly, in the presence of *il12rb1*$^{-/-}$ T cells, *il12rb1*$^{+/+}$ T cells increase their own expression of IFN-γ. The mechanism behind this and its significance to TB control will be a focus of future investigations.

Given the propensity of *IL12RB1* null individuals to develop disseminated forms of mycobacterial disease, we found it very

interesting that *M. tuberculosis* is more readily found near sites of potential dissemination in *il12rb1*$^{-/-}$ mice than in *il12rb1*$^{+/+}$ controls. This was independent of bacterial burden, as localization in/near the vascular and airway epithelia was observed as early as day 20 postinfection in *il12rb1*$^{-/-}$ lungs (at this time, bacterial burdens were equivalent between *il12rb1*$^{+/+}$ and *il12rb1*$^{-/-}$ mice, independent of the homogenization method utilized) (Fig. 1A and data not shown). Regarding the identity of the IL-12 family member promoting this containment, it is likely that IL-12 itself, rather than IL-23 or IL-12(p40)$_2$, is the primary cytokine promoting *M. tuberculosis* containment, given the well-known role IL-12 has in promoting T-cell expression of IFN-γ, which itself can directly activate nonhematopoietic lineages to restrict pathogen growth (21, 50). However, as is clear from the different phenotypes of *M. tuberculosis*-infected *il12b*$^{-/-}$ mice [which lack the IL-12p40 subunit required for IL-12, IL-23, and IL-12(p40)$_2$ activity] and *il12a*$^{-/-}$ mice (which lack the IL-12p35 subunit required for IL-12 and IL-35 activity) (13), the loss of IL-12-signaling alone does not fully explain the phenotype of *il12rb1*$^{-/-}$ mice as reported here. Thus, while IL-12 may be the primary cytokine promoting *M. tuberculosis* containment in the C57BL/6 model (34), what we observe in *il12rb1*$^{-/-}$ mice reflects the concomitant loss of IL-12, IL-23, and IL-12(p40)$_2$ bioactivities. Each of these cytokines is host protective in the context of experimental tuberculosis (23, 27, 32, 34).

IFN-γ is well established as being essential for controlling *M. tuberculosis* infection (12, 22) and is expressed by multiple leukocyte subsets during experimental TB (Fig. 6C). In contrast to the recent suggestion of Sharma et al. (61), flow cytometric analysis of Yeti lungs did not demonstrate CD45^{neg} cells to be a source of IFN-γ during experimental TB (Fig. 6B). Regarding the specific role of T-cell IFN-γ, radiation bone marrow chimeras demonstrate that IFN-γ produced by T cells does significantly contribute to the control of primary *M. tuberculosis* infection. These results complement those of Gallegos et al. (24), who demonstrated that adoptive transfer of *ex vivo* differentiated T cells prior to infection provides protection that is independent of IFN-γ up to 20 days following infection. That experimental approach, which is shared by other laboratories investigating which cytokines T cells must express for pathogen control (65), is fundamentally a vaccination protocol; the animals used in our study are not exposed to *M. tuberculosis* antigens prior to their infection. Consequently, the study by Gallegos et al. (24) is important for future investigations of *M. tuberculosis* vaccination (70). It has been demonstrated that the relative contribution CD4$^+$ and CD8$^+$ T cells make to the total level of IFN-γ expressed during experimental TB fluctuates depending on the stage of infection examined (35). The mechanisms driving this flux have yet to be completely defined, but they are possibly related to variation in the level of *M. tuberculosis* antigens present during different stages of infection (35). Nevertheless, chimeras in which *ifng* deficiency was restricted to *rag1*-dependent cells (i.e., T/B^{ifngKO} mice) did not fully recapitulate the phenotype of either *ifng*$^{-/-}$ mice or *rag1*$^{-/-}$ chimeras reconstituted with *ifng*$^{-/-}$ bone marrow. The simplest explanation for these data is that *rag1*-independent lineages (e.g., NK cells and granulocytes) are an additional source of protective *ifng* during experimental TB. This conclusion is supported by previous comparisons of *M. tuberculosis*-infected *rag1*$^{-/-}$ and *ifng*$^{-/-}$ mice (46) and suggests that the phenotype of T/B^{il12rb1KO} mice is not solely due to impaired *ifng* expression but, rather, reflects a lack of multiple effector mechanisms (Fig. 10).

Less certain still is the role that each individual *IL12RB1* isoform plays in controlling *M. tuberculosis* infection in both humans and the mouse model. Human *IL12RB1* and mouse *il12rb1* produce at least two unique isoforms (56), only one of which has been fully described (i.e., isoform 1, or IL-12Rβ1) (11, 51). The second isoform (i.e., isoform 2, or IL-12Rβ1ΔTM) is the result of alternative splicing (56) and contains a C-terminal sequence that is unlike that of isoform 1. To date, the function of isoform 2 has been examined only in the context of dendritic cell function (56). However, given our demonstration here that *il12rb1* must be expressed by T cells (and not dendritic cells) for TB control to occur, the impetus now should be to determine the relative functions each *il12rb1* isoform has specifically in αβ-T-cell lineages. Since the *il12rb1* knockout mouse used in this study is deficient in both of these isoforms (due to the genomic location at which *neo* is inserted [74]), such investigations will be greatly assisted by the generation of a mouse deficient in only isoform 2.

Finally, it is worth noting that our results do not rule out a role for *il12rb1* expression by other cell types, including nonhematopoietic lineages, during latent stages of infection. Latent TB is the form of disease that the majority of *M. tuberculosis*-infected individuals have and can be modeled in mice using either the low-dose aerogenic infection or Cornell model (38, 59, 62). Using radiation bone marrow chimeras of *ifngr*$^{-/-}$ mice reconstituted with *ifngr*$^{+/+}$ bone marrow, Desvignes and Ernst (17) recently used the low-dose model to demonstrate that nonhematopoietic IFN-γR expression regulates the development of pulmonary immunopathology during latent *M. tuberculosis* infection. This important phenotype is otherwise masked, given the more dominant role hematopoietic IFN-γR expression plays in the early stages of *M. tuberculosis* infection (17). Nonhematopoietic lineages are the most abundant cell type in the lung and, at least in the absence of *il12rb1*, clearly come into contact with *M. tuberculosis* (Fig. 2B). Bronchial epithelia have been demonstrated to express IL-12R, while type II pneumocytes express markers of stress during pulmonary tuberculosis (29). Whether nonhematopoietic lineages in the lungs of humans and mice express *il12rb1* during latent infection, as well as whether the isoforms produced by this gene contribute to immunopathogenesis during latent *M. tuberculosis* infection, is under investigation.

ACKNOWLEDGMENTS

We thank Diane Rodi (Medical College of Wisconsin) for sharing her biosafety expertise while establishing our animal biosafety level 3/biosafety level 3 (ABSL3/BSL3) laboratory. We also thank Dara Frank and Thomas Zahrt of the MCW Center for Infectious Disease Research for sharing their ABSL3/BSL3 laboratory space with us prior to our setting up our own ABSL3/BSL3 laboratory.

This work was supported by the MCW, the MCW Center for Infectious Disease Research, and Advancing Healthier Wisconsin Grant 5520189.

REFERENCES

1. **Airoldi I, et al.** 2009. IL-12 can target human lung adenocarcinoma cells and normal bronchial epithelial cells surrounding tumor lesions. PLoS One **4**:e6119. doi:10.1371/journal.pone.0006119.
2. **Akahoshi M, et al.** 2003. Influence of interleukin-12 receptor beta 1 polymorphisms on tuberculosis. Hum. Genet. **112**:237–243.
3. **Al-Muhsen S, Casanova JL.** 2008. The genetic heterogeneity of Mende-

lian susceptibility to mycobacterial diseases. J. Allergy Clin. Immunol. **122**:1043–1053.
4. **Altare F, et al.** 1998. Impairment of mycobacterial immunity in human interleukin-12 receptor deficiency. Science **280**:1432–1435.
5. **Behar SM, Dascher CC, Grusby MJ, Wang CR, Brenner MB.** 1999. Susceptibility of mice deficient in CD1D or TAP1 to infection with *Mycobacterium tuberculosis*. J. Exp. Med. **189**:1973–1980.
6. **Bharath S, Balasubramanian V.** 2011. Pulmonary tuberculosis in the mouse, p 175–193. *In* Leong FJ, Dartois V, Dick T (ed), A color atlas of comparative pathology of pulmonary tuberculosis. CRC Press, Boca Raton, FL.
7. **Bookout AL, Cummins CL, Mangelsdorf DJ, Pesola JM, Kramer MF.** 2006. High-throughput real-time quantitative reverse transcription PCR. Curr. Protoc. Mol. Biol., **chapter 15**, unit 15.18. doi:10.1002/0471142727.mb1508s73.
8. **Bosco N, Swee LK, Benard A, Ceredig R, Rolink A.** 2010. Auto-reconstitution of the T-cell compartment by radioresistant hematopoietic cells following lethal irradiation and bone marrow transplantation. Exp. Hematol. **38**:222–232.e.2. http://www.exphem.org/article/S0301-472X(09)00487-1/fulltext.
9. **Bussolati B, et al.** 1998. Platelet-activating factor synthesized by IL-12-stimulated polymorphonuclear neutrophils and NK cells mediates chemotaxis. J. Immunol. **161**:1493–1500.
10. **Chua AO, et al.** 1994. Expression cloning of a human IL-12 receptor component. A new member of the cytokine receptor superfamily with strong homology to gp130. J. Immunol. **153**:128–136.
11. **Chua AO, Wilkinson VL, Presky DH, Gubler U.** 1995. Cloning and characterization of a mouse IL-12 receptor-beta component. J. Immunol. **155**:4286–4294.
12. **Cooper AM, et al.** 1993. Disseminated tuberculosis in interferon gamma gene-disrupted mice. J. Exp. Med. **178**:2243–2247.
13. **Cooper AM, et al.** 2002. Mice lacking bioactive IL-12 can generate protective, antigen-specific cellular responses to mycobacterial infection only if the IL-12 p40 subunit is present. J. Immunol. **168**:1322–1327.
14. **de Beaucoudrey L, et al.** 2008. Mutations in STAT3 and IL12RB1 impair the development of human IL-17-producing T cells. J. Exp. Med. **205**:1543–1550.
15. **de Beaucoudrey L, et al.** 2010. Revisiting human IL-12Rbeta1 deficiency: a survey of 141 patients from 30 countries. Medicine (Baltimore) **89**:381–402.
16. **de Jong R, et al.** 1998. Severe mycobacterial and Salmonella infections in interleukin-12 receptor-deficient patients. Science **280**:1435–1438.
17. **Desvignes L, Ernst JD.** 2009. Interferon-gamma-responsive nonhematopoietic cells regulate the immune response to *Mycobacterium tuberculosis*. Immunity **31**:974–985.
18. **D'Souza CD, et al.** 2000. A novel nonclassic beta2-microglobulin-restricted mechanism influencing early lymphocyte accumulation and subsequent resistance to tuberculosis in the lung. Am. J. Respir. Cell Mol. Biol. **23**:188–193.
19. **Dunn PL, North RJ.** 1995. Virulence ranking of some *Mycobacterium tuberculosis* and *Mycobacterium bovis* strains according to their ability to multiply in the lungs, induce lung pathology, and cause mortality in mice. Infect. Immun. **63**:3428–3437.
20. **Ekkens MJ, et al.** 2007. Th1 and Th2 cells help CD8 T-cell responses. Infect. Immun. **75**:2291–2296.
21. **Evans SE, et al.** 2010. Stimulated innate resistance of lung epithelium protects mice broadly against bacteria and fungi. Am. J. Respir. Cell Mol. Biol. **42**:40–50.
22. **Flynn JL, et al.** 1993. An essential role for interferon gamma in resistance to *Mycobacterium tuberculosis* infection. J. Exp. Med. **178**:2249–2254.
23. **Flynn JL, et al.** 1995. IL-12 increases resistance of BALB/c mice to *Mycobacterium tuberculosis* infection. J. Immunol. **155**:2515–2524.
24. **Gallegos AM, et al.** 2011. A gamma interferon independent mechanism of CD4 T cell mediated control of *M. tuberculosis* infection in vivo. PLoS Pathog. **7**:e1002052. doi:10.1371/journal.ppat.1002052.
25. **Guia S, et al.** 2008. A role for interleukin-12/23 in the maturation of human natural killer and $CD56^+$ T cells in vivo. Blood **111**:5008–5016.
26. **Guler ML, et al.** 1996. Genetic susceptibility to *Leishmania*: IL-12 responsiveness in TH1 cell development. Science **271**:984–987.
27. **Holscher C, et al.** 2001. A protective and agonistic function of IL-12p40 in mycobacterial infection. J. Immunol. **167**:6957–6966.
28. **Hsieh CS, et al.** 1993. Development of TH1 $CD4^+$ T cells through IL-12 produced by *Listeria*-induced macrophages. Science **260**:547–549.
29. **Inoue Y, et al.** 1995. Evaluation of serum KL-6 levels in patients with pulmonary tuberculosis. Tuber Lung Dis. **76**:230–233.
30. **Johnson CM, et al.** 1997. *Mycobacterium tuberculosis* aerogenic rechallenge infections in B cell-deficient mice. Tuber Lung Dis. **78**:257–261.
31. **Khader SA, et al.** 2007. IL-23 and IL-17 in the establishment of protective pulmonary $CD4^+$ T cell responses after vaccination and during *Mycobacterium tuberculosis* challenge. Nat. Immunol. **8**:369–377.
32. **Khader SA, et al.** 2011. IL-23 is required for long-term control of *Mycobacterium tuberculosis* and B cell follicle formation in the infected lung. J. Immunol. **187**:5402–5407.
33. **Khader SA, et al.** 2006. Interleukin 12p40 is required for dendritic cell migration and T cell priming after *Mycobacterium tuberculosis* infection. J. Exp. Med. **203**:1805–1815.
34. **Khader SA, et al.** 2005. IL-23 compensates for the absence of IL-12p70 and is essential for the IL-17 response during tuberculosis but is dispensable for protection and antigen-specific IFN-gamma responses if IL-12p70 is available. J. Immunol. **175**:788–795.
35. **Lazarevic V, Nolt D, Flynn JL.** 2005. Long-term control of *Mycobacterium tuberculosis* infection is mediated by dynamic immune responses. J. Immunol. **175**:1107–1117.
36. **Ma CS, et al.** 2012. Functional STAT3 deficiency compromises the generation of human T follicular helper cells. Blood **119**:3997–4008.
37. **Marquis JF, et al.** 2008. Fibrotic response as a distinguishing feature of resistance and susceptibility to pulmonary infection with Mycobacterium tuberculosis in mice. Infect. Immun. **76**:78–88.
38. **McCune RM, Feldmann FM, Lambert HP, McDermott W.** 1966. Microbial persistence. I. The capacity of tubercle bacilli to survive sterilization in mouse tissues. J. Exp. Med. **123**:445–468.
39. **Metzger DW, et al.** 1997. Interleukin-12 acts as an adjuvant for humoral immunity through interferon-gamma-dependent and -independent mechanisms. Eur. J. Immunol. **27**:1958–1965.
40. **Meyts I, et al.** 2006. IL-12 contributes to allergen-induced airway inflammation in experimental asthma. J. Immunol. **177**:6460–6470.
41. **Mogues T, Goodrich ME, Ryan L, LaCourse R, North RJ.** 2001. The relative importance of T cell subsets in immunity and immunopathology of airborne *Mycobacterium tuberculosis* infection in mice. J. Exp. Med. **193**:271–280.
42. **Mohan K, Stevenson MM.** 1998. Dyserythropoiesis and severe anaemia associated with malaria correlate with deficient interleukin-12 production. Br. J. Haematol. **103**:942–949.
43. **Mohan K, Stevenson MM.** 1998. Interleukin-12 corrects severe anemia during blood-stage *Plasmodium chabaudi* AS in susceptible A/J. mice. Exp. Hematol. **26**:45–52.
44. **Moreno SE, et al.** 2006. IL-12, but not IL-18, is critical to neutrophil activation and resistance to polymicrobial sepsis induced by cecal ligation and puncture. J. Immunol. **177**:3218–3224.
45. **North RJ.** 1973. Importance of thymus-derived lymphocytes in cell-mediated immunity to infection. Cell Immunol. **7**:166–176.
46. **North RJ, Jung YJ.** 2004. Immunity to tuberculosis. Annu. Rev. Immunol. **22**:599–623.
47. **Oppmann B, et al.** 2000. Novel p19 protein engages IL-12p40 to form a cytokine, IL-23, with biological activities similar as well as distinct from IL-12. Immunity **13**:715–725.
48. **Ordway DJ, Orme IM.** 2011. Animal models of mycobacteria infection. Curr. Protoc. Immunol., chapter 19, unit 19.15. doi:10.1002/0471142735.im1905s94.
49. **Pearce EL, Shen H.** 2007. Generation of CD8 T cell memory is regulated by IL-12. J. Immunol. **179**:2074–2081.
50. **Pfefferkorn ER.** 1984. Interferon gamma blocks the growth of *Toxoplasma gondii* in human fibroblasts by inducing the host cells to degrade tryptophan. Proc. Natl. Acad. Sci. U. S. A. **81**:908–912.
51. **Presky DH, et al.** 1996. A functional interleukin 12 receptor complex is composed of two beta-type cytokine receptor subunits. Proc. Natl. Acad. Sci. U. S. A. **93**:14002–14007.
52. **Reiley WW, et al.** 2008. ESAT-6-specific CD4 T cell responses to aerosol *Mycobacterium tuberculosis* infection are initiated in the mediastinal lymph nodes. Proc. Natl. Acad. Sci. U. S. A. **105**:10961–10966.
53. **Reiley WW, et al.** 2010. Distinct functions of antigen-specific CD4 T cells during murine *Mycobacterium tuberculosis* infection. Proc. Natl. Acad. Sci. U. S. A. **107**:19408–19413.
54. **Reinhardt RL, Hong S, Kang SJ, Wang ZE, Locksley RM.** 2006. Visualization of IL-12/23p40 in vivo reveals immunostimulatory dendritic cell migrants that promote Th1 differentiation. J. Immunol. **177**:1618–1627.

55. **Rhoades ER, Frank AA, Orme IM.** 1997. Progression of chronic pulmonary tuberculosis in mice aerogenically infected with virulent *Mycobacterium tuberculosis*. Tuber. Lung Dis. **78**:57–66.
56. **Robinson RT, et al.** 2010. *Mycobacterium tuberculosis* infection induces il12rb1 splicing to generate a novel IL-12Rβ1 isoform that enhances DC migration. J. Exp. Med. **207**:591–605.
57. **Russell DG, Barry CE, III, Flynn JL.** 2010. Tuberculosis: what we don't know can, and does, hurt us. Science **328**:852–856.
58. **Russell TD, et al.** 2003. IL-12 p40 homodimer-dependent macrophage chemotaxis and respiratory viral inflammation are mediated through IL-12 receptor beta 1. J. Immunol. **171**:6866–6874.
59. **Scanga CA, et al.** 1999. Reactivation of latent tuberculosis: variations on the Cornell murine model. Infect. Immun. **67**:4531–4538.
60. **Schneider E, Tonanny MB, Lisbonne M, Leite-de-Moraes M, Dy M.** 2004. Pro-Th1 cytokines promote Fas-dependent apoptosis of immature peripheral basophils. J. Immunol. **172**:5262–5268.
61. **Sharma M, Sharma S, Roy S, Varma S, Bose M.** 2007. Pulmonary epithelial cells are a source of interferon-gamma in response to *Mycobacterium tuberculosis* infection. Immunol. Cell Biol. **85**:229–237.
62. **Shi C, Shi J, Xu Z.** 2011. A review of murine models of latent tuberculosis infection. Scand. J. Infect. Dis. **43**:848–856.
63. **Showe LC, et al.** 1996. Structure of the mouse IL-12R beta 1 chain and regulation of its expression in BCG/LPS-treated mice. Ann. N. Y. Acad. Sci. **795**:413–415.
64. **Stetson DB, et al.** 2003. Constitutive cytokine mRNAs mark natural killer (NK) and NK T cells poised for rapid effector function. J. Exp. Med. **198**:1069–1076.
65. **Strutt TM, et al.** 2010. Memory $CD4^+$ T cells induce innate responses independently of pathogen. Nat. Med. **16**:558–564.
66. **Sugawara I, et al.** 2002. Mycobacterial infection in natural killer T cell knockout mice. Tuberculosis (Edinb.) **82**:97–104.
67. **Sullivan BM, Juedes A, Szabo SJ, von Herrath M, Glimcher LH.** 2003. Antigen-driven effector CD8 T cell function regulated by T-bet. Proc. Natl. Acad. Sci. U. S. A. **100**:15818–15823.
68. **Szabo SJ, Sullivan BM, Peng SL, Glimcher LH.** 2003. Molecular mechanisms regulating Th1 immune responses. Annu. Rev. Immunol. **21**:713–758.
69. **Taha RA, et al.** 1999. Increased expression of IL-12 receptor mRNA in active pulmonary tuberculosis and sarcoidosis. Am. J. Respir. Crit. Care Med. **160**:1119–1123.
70. **Torrado E, Cooper AM.** 2011. What do we really know about how CD4 T cells control *Mycobacterium tuberculosis*? PLoS Pathog. **7**:e1002196. doi:10.1371/journal.ppat.1002196.
71. **Ueta C, et al.** 1996. Interleukin-12 activates human gamma delta T cells: synergistic effect of tumor necrosis factor-alpha. Eur. J. Immunol. **26**:3066–3073.
72. **Wang X, et al.** 1999. Characterization of mouse interleukin-12 p40 homodimer binding to the interleukin-12 receptor subunits. Eur. J. Immunol. **29**:2007–2013.
73. **Watford WT, Moriguchi M, Morinobu A, O'Shea JJ.** 2003. The biology of IL-12: coordinating innate and adaptive immune responses. Cytokine Growth Factor Rev. **14**:361–368.
74. **Wu C, Ferrante J, Gately MK, Magram J.** 1997. Characterization of IL-12 receptor β1 chain (IL-12Rβ1)-deficient mice: IL-12Rβ1 is an essential component of the functional mouse IL-12 receptor. J. Immunol. **159**:1658–1665.
75. **Zhang H, et al.** 2007. Modulation of mast cell proteinase-activated receptor expression and IL-4 release by IL-12. Immunol. Cell Biol. **85**:558–566.